Chapter 3
Theory for Thermal Wave Control: Transformation Complex Thermotics

Abstract In this chapter, we develop a transformation theory for controlling wave-like temperature fields (called thermal waves herein) in conduction and advection. We first unify these two basic heat transfer modes by coining a complex thermal conductivity whose real and imaginary parts are related to conduction and advection. Consequently, the conduction-advection process supporting thermal waves is described by a complex conduction equation, thus called complex thermotics. We then propose the principle for transforming complex thermal conductivities. We further design three metamaterials to control thermal waves with cloaking, concentrating, and rotating functions. Experimental suggestions are also provided based on porous media.

Keywords Transformation complex thermotics · Thermal waves · Porous media

3.1 Opening Remarks

Conduction and advection are ubiquitous, with crucial parameters of thermal conductivities and advection velocities, respectively. Therefore, these two heat transfer modes are generally considered independent, challenging their simultaneous manipulation. Recently, transformation theories have been proposed to control conduction and advection simultaneously, yielding practical applications such as cloaking, concentrating, and rotating [1–3]. These theories apply to constant-temperature boundary conditions but are not necessarily appropriate for periodic boundary conditions supporting thermal waves.

To solve the problem, we resort to a complex thermal conductivity $\kappa = \sigma + \mathrm{i}\tau$, where σ and τ are two real numbers [4]. The κ can be well understood with the complex plane shown in Fig. 3.1. We consider thermal waves with rightward advection velocities. The temperature profiles in the right ($\sigma > 0$) and left ($\sigma < 0$) half-planes have loss and gain of heat energy, respectively. The motion of the temperature profiles in the upper ($\tau > 0$) and lower ($\tau < 0$) half-planes is rightward and leftward, respectively. Therefore, the conduction-advection process supporting thermal waves can be described by a complex conduction equation, thus called complex thermotics

L.-J. Xu and J.-P. Huang, *Transformation Thermotics and Extended Theories*,
https://doi.org/10.1007/978-981-19-5908-0_3

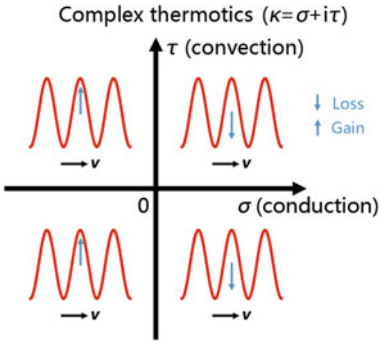

Fig. 3.1 Connotation of the complex thermal conductivity $\kappa = \sigma + \mathrm{i}\tau$. Red curves denote thermal waves. Advection velocities are rightward. The arrow in the center of each temperature profile indicates loss or gain. Adapted from Ref. [6]

herein. In other words, advection can be regarded as a complex form of conduction. Transforming complex materials was also realized in wave systems with a similar idea [5], where gain/loss leads to non-Hermitian dielectrics.

We further study the complex conduction equation and propose the theory of transformation complex thermotics, linking spatial transformations and material transformations. We first prove the form-invariance of the complex conduction equation under coordinate transformations and derive the principle for transforming complex thermal conductivities. The present theory further allows us to cloak, concentrate, and rotate thermal waves as three model applications. Specifically, cloaking can hide an obstacle without distorting the thermal waves in the background; concentrating can enhance the density of thermal waves; rotating can control the direction of thermal waves. We further provide experimental suggestions based on porous media whose effective parameters can be calculated by weighted average.

3.2 Theoretical Foundation

Complex thermotics can be described by a complex conduction equation,

$$\rho C \frac{\partial T}{\partial t} + \nabla \cdot (-\kappa \nabla T) = 0, \tag{3.1}$$

where ρ, C, κ, T, and t are density, heat capacity, complex thermal conductivity, temperature, and time, respectively. The complex thermal conductivity κ can be expressed as [4]

$$\kappa = \sigma + \mathrm{i}\tau = \sigma + \mathrm{i}\frac{\rho C \boldsymbol{v} \cdot \boldsymbol{\beta}}{\beta^2}, \tag{3.2}$$

where $\boldsymbol{v}$ is advection velocity, and $\boldsymbol{\beta}$ is wave vector. By applying a wavelike temperature field [7, 8] described by $T = A_0 \mathrm{e}^{\mathrm{i}(\boldsymbol{\beta}\cdot\boldsymbol{r}-\omega t)} + T_0$, we can derive the dispersion relation of complex thermotics,

$$\omega = \boldsymbol{v} \cdot \boldsymbol{\beta} - \mathrm{i}\frac{\sigma\beta^2}{\rho C}, \tag{3.3}$$

where A_0, $\boldsymbol{r}$, ω, and T_0 are the amplitude, position vector, angular frequency, and reference temperature of the wavelike temperature field, respectively. The wavelike temperature field can also be called a thermal wave because it mathematically corresponds to a plane wave. Note that thermal waves herein have a distinct mechanism from those thermal-relaxation-related heat waves [9, 10]. Equation (3.2) is a mathematical skill to unify conduction and advection. Due to the feature of thermal waves (say, $\nabla T = \mathrm{i}\boldsymbol{\beta} T$), we can derive $\mathrm{i}\tau \cdot \nabla T = -\tau\boldsymbol{\beta} T$ which just corresponds to an advection term.

We then prove that the complex conduction equation (Eq. (3.1)) is form-invariant under the spatial transformation from a curvilinear space X to a physical space X'. For this purpose, we rewrite Eq. (3.1) as

$$\rho C\frac{\partial T}{\partial t} + \nabla \cdot (-\sigma \nabla T) + \nabla \cdot (\tau \boldsymbol{\beta} T) = 0. \tag{3.4}$$

We suppose $\boldsymbol{u} = \tau\boldsymbol{\beta}$ and write down the component form of Eq. (3.4) in the curvilinear space with a contravariant basis $\left(\boldsymbol{g}^1,\ \boldsymbol{g}^2,\ \boldsymbol{g}^3\right)$ and contravariant components $\left(x^1,\ x^2,\ x^3\right)$,

$$\sqrt{g}\rho C\partial_t T + \partial_j\left(-\sqrt{g}\sigma^{jk}\partial_k T\right) + \partial_j\left(\sqrt{g}u^j T\right) = 0, \tag{3.5}$$

where g is the determinant of the matrix $\boldsymbol{g}_j \cdot \boldsymbol{g}_k$ with $(\boldsymbol{g}_1,\ \boldsymbol{g}_2,\ \boldsymbol{g}_3)$ being a covariant basis, and j (or k) takes 1, 2 or 3. Equation (3.5) is expressed in the curvilinear space, and then we rewrite it in the physical space with Cartesian coordinates $\left(x^{1'},\ x^{2'},\ x^{3'}\right)$,

$$\sqrt{g}\rho C\partial_t T + \partial_{j'}\frac{\partial x^{j'}}{\partial x^j}\left(-\sqrt{g}\sigma^{jk}\frac{\partial x^{k'}}{\partial x^k}\partial_{k'} T\right) + \partial_{j'}\frac{\partial x^{j'}}{\partial x^j}\left(\sqrt{g}u^j T\right) = 0, \tag{3.6}$$

where $\partial x^{j'}/\partial x^j$ and $\partial x^{k'}/\partial x^k$ are the components of the Jacobian transformation matrix $\tilde{J}$, and $\sqrt{g} = 1/\det\tilde{J}$. We turn the spatial transformation into the transformation of materials or vectors, so Eq. (3.6) becomes

$$\frac{\rho C}{\det\tilde{J}}\partial_t T + \partial_{j'}\left(-\frac{\frac{\partial x^{j'}}{\partial x^j}\sigma^{jk}\frac{\partial x^{k'}}{\partial x^k}}{\det\tilde{J}}\partial_{k'} T\right) + \partial_{j'}\left(\frac{\frac{\partial x^{j'}}{\partial x^j}u^j}{\det\tilde{J}}T\right) = 0. \tag{3.7}$$

The transformation rule can be derived,

$$(\rho C)' = \frac{\rho C}{\det\tilde{J}}, \tag{3.8a}$$

$$\sigma' = \frac{\tilde{J}\sigma\tilde{J}^{\dagger}}{\det\tilde{J}}, \tag{3.8b}$$

$$\boldsymbol{u}' = \frac{\tilde{J}\boldsymbol{u}}{\det\tilde{J}}, \tag{3.8c}$$

where $\tilde{J}^{\dagger}$ represents the transpose of $\tilde{J}$. Since $\boldsymbol{u} = \tau\boldsymbol{\beta}$, Eq. (3.8c) becomes

$$(\tau\boldsymbol{\beta})' = \frac{\tilde{J}(\tau\boldsymbol{\beta})}{\det\tilde{J}}. \tag{3.9}$$

We do not transform the wave vector, i.e., $\boldsymbol{\beta}' = \boldsymbol{\beta}$, so Eq. (3.9) turns into

$$\tau' = \frac{\tilde{J}\tau}{\det\tilde{J}}. \tag{3.10}$$

Therefore, the principle for transforming complex thermal conductivities can be summarized as

$$(\rho C)' = \frac{\rho C}{\det\tilde{J}}, \tag{3.11a}$$

$$\sigma' = \frac{\tilde{J}\sigma\tilde{J}^{\dagger}}{\det\tilde{J}}, \tag{3.11b}$$

$$\tau' = \frac{\tilde{J}\tau}{\det\tilde{J}}. \tag{3.11c}$$

Equation (3.11) is the first key result, acting as the foundation of transformation complex thermotics. Physically, Eqs. (3.11a) and (3.11b) agree with the result given by the theory of transformation thermotics for conduction [11, 12]. A crucial point is to show that Eq. (3.11c) does not violate physical laws either. For this purpose, we substitute the expression of τ (Eq. (3.2)) into Eq. (3.11c), thus yielding

$$\left(\frac{\rho C\boldsymbol{v}\cdot\boldsymbol{\beta}}{\beta^2}\right)' = \frac{\tilde{J}\left(\frac{\rho C\boldsymbol{v}\cdot\boldsymbol{\beta}}{\beta^2}\right)}{\det\tilde{J}}. \tag{3.12}$$

With Eq. (3.11a) and $\boldsymbol{\beta}' = \boldsymbol{\beta}$, Eq. (3.12) can be reduced to

$$\boldsymbol{v}' = \tilde{J}\boldsymbol{v}, \tag{3.13}$$

which also agrees with the theory of transformation thermotics for advection [1–3]. Therefore, we may briefly summarize two conclusions: (I) complex thermotics indicates that the real and imaginary parts of a complex thermal conductivity (Eq. (3.2)) are related to conduction (featuring dissipation) and advection (featuring propaga-

tion), respectively; and (II) the governing equation of complex thermotics (Eq. (3.1)) is form-invariant under coordinate transformations.

3.3 Model Application

The form-invariance of the complex conduction equation (Eq. (3.1)) allows us to cloak, concentrate, and rotate thermal waves. A schematic diagram of cloaking is shown in Fig. 3.2a. The left and right ends are set with periodic boundary conditions, say, $T_L = T_R$. The upper and lower boundaries are insulated. We consider the case with $\boldsymbol{v}//\boldsymbol{\beta}$ where the imaginary part of κ appears, as calculated by Eq. (3.2). We take on the wave vector $\beta = 2\pi m/W$ with $m = 10$, and the time period of the thermal wave is $t_0 = 20$ s according to Eq. (3.3). We set the initial wavelike temperature field as $T = 40\sin(\beta x) + 323$ K (Fig. 3.2b). When there is an obstacle without motion in the center, the thermal wave is distorted (Fig. 3.2c and d). Different from the schemes with analytical design [13–15] and topological optimization [16–19], we apply the present theory of transformation complex thermotics to design thermal cloaking. The coordinate transformation can be expressed as $r = ar' + b$ and $\theta = \theta'$, where (r, θ) denote cylindrical coordinates in the physical space, $a = (r_2 - r_1)/r_2$, and $b = r_1$. Here, r_1 and r_2 are the inner and outer radii of the shell, respectively. The Jacobian transformation matrix $\tilde{J}$ can be calculated as $\tilde{J} = \mathrm{diag}[a,\ ar/(r-b)]$. We design the cloak according to Eq. (3.11). The initial wavelike temperature field in the cloak turns into $T = 40\sin\{\beta[(r-b)x/(ar)]\} + 323$ K (Fig. 3.2e). Here, the wave vector β is not transformed indeed, and only the coordinate x becomes $(r-b)x/(ar)$. The obstacle does not distort the thermal wave in the background, so the cloaking effect is achieved (Fig. 3.2f and g). Since the dispersion relation (Eq. (3.3)) indicates that the decay rate (-Im(ω)) is in direct proportion to thermal conductivity, the temperature of the obstacle (with a high thermal conductivity of 120 W m^{-1} K^{-1}) decays quickly and becomes a constant. Meanwhile, the thermal wave has energy loss due to the positive real part of κ, and propagates rightwards along x axis due to the positive imaginary part of κ. After propagating for one period (20 s), the thermal wave approximately gains a phase difference of 2π, thus going back to the initial position (Fig. 3.2e and g).

With the similar method for cloaking, we can also design concentrating and rotating. The transformation of concentrating is $r = cr'$ for $0 < r' < r_m$, $r = dr' + f$ for $r_m < r' < r_2$, and $\theta = \theta'$. Here, $c = r_1/r_m$, $d = (r_2 - r_1)/(r_2 - r_m)$, $f = (r_1 - r_m)r_2/(r_2 - r_m)$, and r_m is an intermediate radius between r_1 and r_2. The concentrating effect is determined by the parameter $1/c = r_m/r_1$, whose maximum value is r_2/r_1. Therefore, increasing the value of r_m can enhance the thermal gradient inside the concentrator. We can derive the Jacobian matrix $\tilde{J}$ in the core as $\tilde{J} = \mathrm{diag}[c,\ c]$, and that for the shell as $\tilde{J} = \mathrm{diag}[d,\ dr/(r-f)]$. The initial wavelike temperature field in the core turns into $T = 40\sin[\beta(x/c)] + 323$ K, and that in the shell becomes $T = 40\sin\{\beta[(r-f)x/(dr)]\} + 323$ K (Fig. 3.3a). The thermal waves

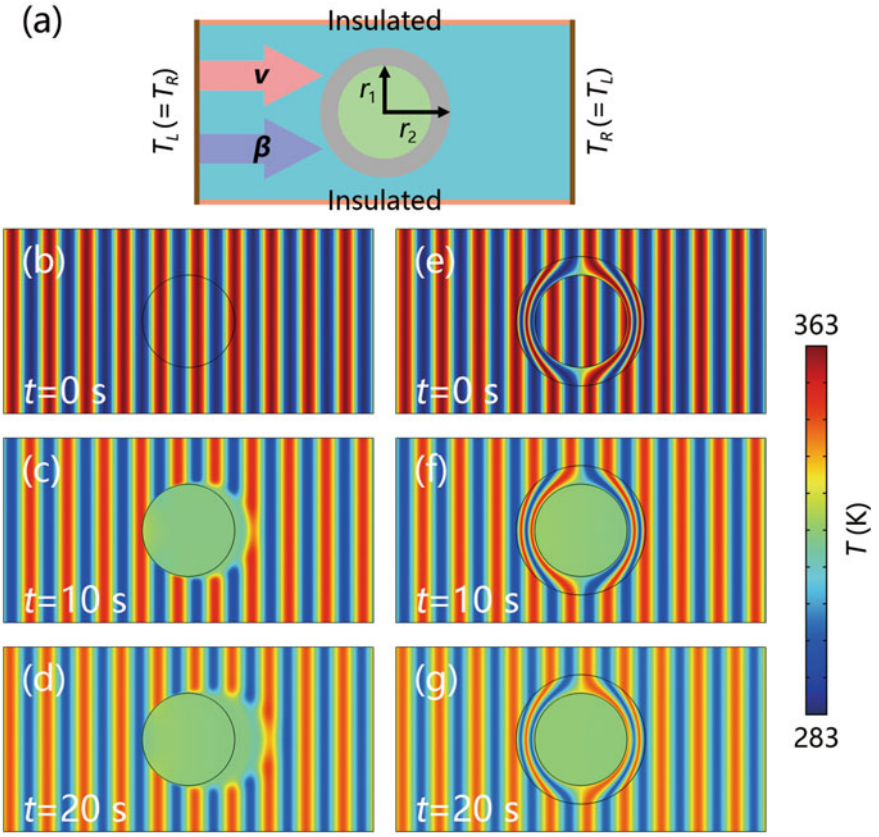

Fig. 3.2 **a** Schematic diagram of cloaking. **b–d** Simulations with an obstacle in the center. **e–g** Simulations with an obstacle coated by a cloak. Background parameters: $W = 20$ cm, $H = 10$ cm, $\rho = 1000$ kg/m^3, $C = 4200$ J kg^{-1} K^{-1}, $\sigma = 0.6$ W m^{-1} K^{-1}, and $v = 0.1$ cm/s. The obstacle is without motion, and has only a different parameter of $\sigma = 120$ W m^{-1} K^{-1} from background parameters. Cloaking parameters: the product of density and heat capacity is $\rho C\,(r-b)\,/\left(a^2 r\right)$; the real part of the complex thermal conductivity is diag $[(r-b)\,\sigma/r,\ r\sigma/\,(r-b)]$; and the velocity is $v\,[a\cos\theta,\ -ar\sin\theta/\,(r-b)]^{\dagger}$ with $r_1 = 2.5$ cm, $r_2 = 3.5$ cm, $a = 2/7$, and $b = 2.5$ cm. Adapted from Ref. [6]

at $t = 10$ s and $t = 20$ s are shown in Fig. 3.3b and c, respectively. The thermal wave in the center is concentrated indeed.

The transformation of rotating is $r = r'$, $\theta = \theta' + \theta_0$ for $0 < r' < r_1$, and $\theta = \theta' + h\,(r - r_2)$ for $r_1 < r' < r_2$. Here, $h = \theta_0/\,(r_1 - r_2)$, and θ_0 is rotating angle. We can derive the Jacobian matrix in the core as $\tilde{J} = \text{diag}\,[1,\ 1]$, and that in the shell as $\tilde{J} = [(1,\ 0)\,,\ (hr,\ 1)]$. The initial wavelike temperature field in the core turns into $T = 40\sin[\beta\,(x\cos\theta_0 + y\sin\theta_0)] + 323$ K, and that in the shell turns into $T = 40\sin\{\beta\,\{x\cos[h\,(r - r_2)] + y\sin[h\,(r - r_2)]\}\} + 323$ K (Fig. 3.3d). The thermal waves at $t = 10$ s and $t = 20$ s are shown in Fig. 3.3e and f, respectively. We

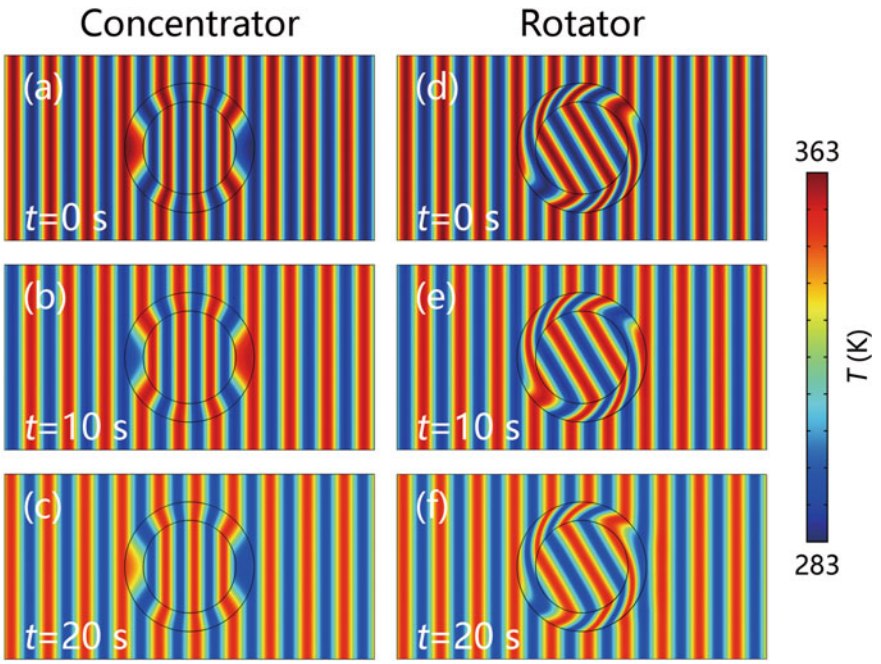

Fig. 3.3 Simulations of **a**–**c** concentrating and **d**–**f** rotating. The system sizes (W, H, r_1, and r_2) and background parameters (ρ, C, σ, and v) are the same as those for Fig. 3.2. Core parameters in **a**–**c**: $\rho C/c^2$, σ, and cv. Shell parameters in **a**–**c**: $\rho C\,(r-f)\,/\left(d^2 r\right)$, $\mathrm{diag}\left[(r-f)\,\sigma/r,\ r\sigma/\,(r-f)\right]$, and $v\,[d\cos\theta,\ -dr\sin\theta/\,(r-f)]^{\dagger}$ with $r_m = 3.2$ cm, $c = 25/32$, $d = 10/3$, and $f = -49/6$ cm. Core parameters in **d**–**f**: ρC, σ, and $v\,[\cos\theta_0,\ \sin\theta_0]^{\dagger}$. Shell parameters in **d**–**f**: ρC, $\sigma\left[(1,\ hr)\,,\ \left(hr,\ h^2r^2+1\right)\right]$, and $v\,[\cos\theta,\ hr\cos\theta-\sin\theta]^{\dagger}$ with $\theta_0 = \pi/6$ rad and $h = -\pi/6$ rad/cm. Adapted from Ref. [6]

can observe that the direction of thermal wave in the center is rotated by $\theta_0 = \pi/6$ anticlockwise.

Here, we only apply a single coordinate transformation to realize a single function. If one combines different coordinate transformations, it is possible to design devices with functions of cloaking-rotating [20] or concentrating-rotating [21]. Certainly, model applications are not limited to the above three devices, and many other applications can also be expected, such as thermal camouflage.

3.4 Experimental Suggestion

The transformation of τ (Eq. (3.11c)) is related to the transformation of $\boldsymbol{v}$ (Eq. (3.13)), which is mathematically easy but experimentally difficult. Meanwhile, we should transform the density and heat capacity of moving media, which is also experimen-

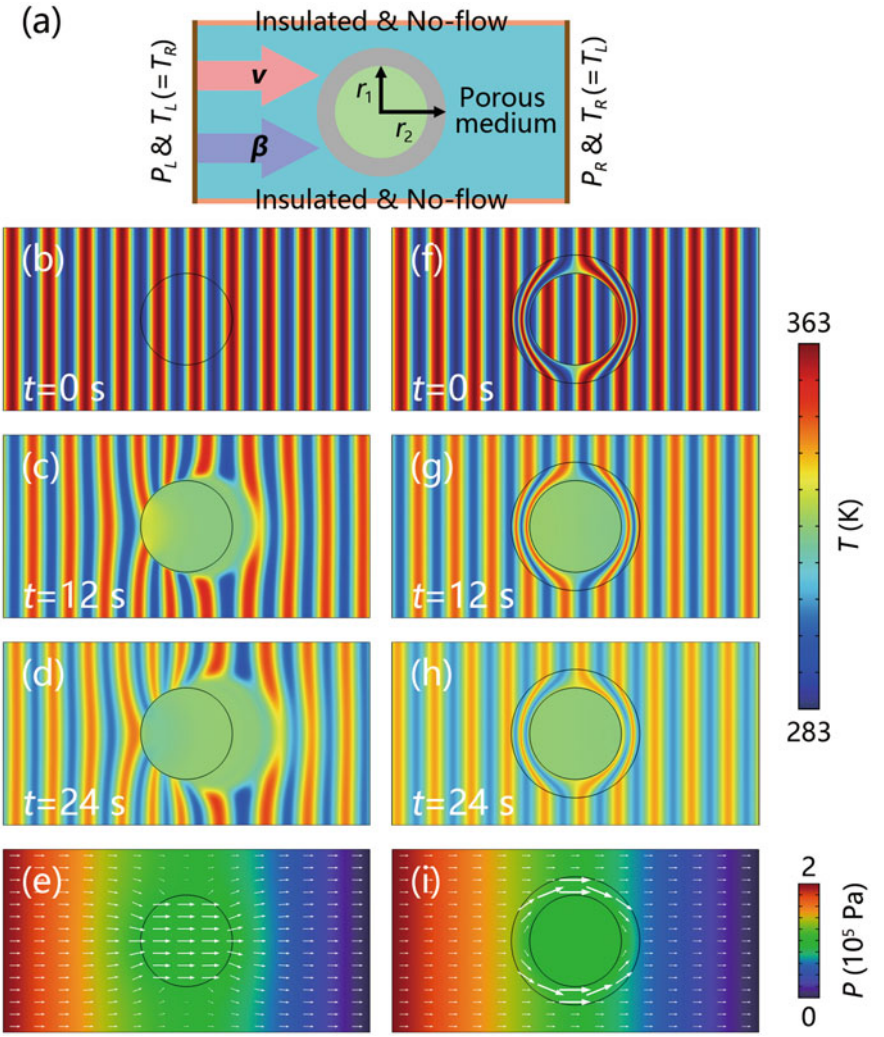

Fig. 3.4 **a** Schematic diagram of cloaking in porous media. **b–d** Temperature profiles and **e** pressure distribution with an obstacle located in the center. **f–h** Temperature profiles and **i** pressure distribution with the same obstacle coated by a cloak. White arrows in **e** and **i** denote advection velocities. $P_L = 2 \times 10^5$ Pa and $P_R = 0$ Pa. The fluid is still water with $\rho_f = 1000$ kg/m^3, $C_f = 4200$ J kg^{-1} K^{-1}, $\sigma_f = 0.6$ W m^{-1} K^{-1}, and $\xi = 10^{-3}$ Pa s. The background solid is stone with parameters $\rho_s = 4000$ kg/m^3, $C_s = 840$ J kg^{-1} K^{-1}, $\sigma_s = 2$ W m^{-1} K^{-1}, $\eta = 10^{-12}$ m^2, and $\phi = 0.8$. The obstacle has only different parameters of $\sigma = 400$ W m^{-1} K^{-1} and $\eta = 2 \times 10^{-10}$ m^2 from the background solid. The parameters in the shell are transformed as Eq. (3.17). Adapted from Ref. [6]

tally difficult. Fortunately, many fluid models can help [22–31]. Here, we utilize porous media [22] to proceed. Then, we should extend transformation complex thermotics from pure materials to composite materials. The porous medium is composed of solid and fluid with solid porosity of ϕ. We denote the density and heat capacity of the solid (or fluid) as ρ_s (or ρ_f) and C_s (or C_f), respectively. The effective density (ρ) and heat capacity (C) of the porous medium can be derived from the weighted average of the solid and fluid, say, $\rho C = \phi\rho_f C_f + (1-\phi)\,\rho_s C_s$. Similar to Eq. (3.2), the complex thermal conductivities of the solid and fluid can be expressed as

$$\kappa_s = \sigma_s + \mathrm{i}\tau_s = \sigma_s + \mathrm{i}\frac{\rho_s C_s \boldsymbol{v}_s \cdot \boldsymbol{\beta}}{\beta^2}, \tag{3.14a}$$

$$\kappa_f = \sigma_f + \mathrm{i}\tau_f = \sigma_f + \mathrm{i}\frac{\rho_f C_f \boldsymbol{v}_f \cdot \boldsymbol{\beta}}{\beta^2}, \tag{3.14b}$$

where $\boldsymbol{v}_s$ and $\boldsymbol{v}_f$ are the velocities of the solid and fluid, respectively. The imaginary part of Eq. (3.14a) generally vanishes ($\tau_s = 0$) when the solid does not move ($\boldsymbol{v}_s = 0$). It is reasonable to handle the real parts of Eq. (3.14) with the method of weighted average, thus yielding the real part of the effective complex thermal conductivity as $\sigma = \phi\sigma_f + (1-\phi)\,\sigma_s$ [32]. The next question is how to handle the imaginary parts of Eq. (3.14). We know that the imaginary part τ of the effective complex thermal conductivity is related to propagation, which has vector property to some extent. Therefore, it is also physical to use the method of weighted average to derive the effective imaginary part, say, $\tau = \phi\tau_f + (1-\phi)\,\tau_s$. Therefore, the effective complex thermal conductivity κ of the porous medium can be expressed as

$$\kappa = \sigma + \mathrm{i}\tau = \phi\sigma_f + (1-\phi)\,\sigma_s + \mathrm{i}\left[\phi\tau_f + (1-\phi)\,\tau_s\right] \equiv \phi\kappa_f + (1-\phi)\,\kappa_s. \tag{3.15}$$

Equation (3.15) is the second key result, describing the effective complex thermal conductivity of composite materials. By substituting Eq. (3.15) into Eq. (3.1), we can obtain the dispersion relation in porous media,

$$\omega = \frac{\phi\rho_f C_f}{\rho C}\boldsymbol{v}_f \cdot \boldsymbol{\beta} + \frac{(1-\phi)\,\rho_s C_s}{\rho C}\boldsymbol{v}_s \cdot \boldsymbol{\beta} - \mathrm{i}\frac{\sigma\beta^2}{\rho C}. \tag{3.16}$$

When $\phi = 1$, the porous medium becomes pure fluid, and Eq. (3.16) is reduced to Eq. (3.3) naturally.

With the understanding of Eq. (3.15), we can still use the result of Eq. (3.11), but it is not enough. We should consider the Darcy law and mass conservation. The Darcy law indicates that the origin of advection velocity is pressure difference, say, $\boldsymbol{v} = -(\eta/\xi)\,\nabla P$ where η is permeability, ξ is dynamic viscosity, and P denotes pressure. Since the pressure field is stable, density does not change with time and mass conservation is satisfied naturally. With these two physical conditions, we can obtain the transformation rule in porous media,

$$\left(\rho_f C_f\right)' = \rho_f C_f, \tag{3.17a}$$

$$\sigma_f' = \sigma_f, \tag{3.17b}$$

$$(\rho_s C_s)' = \frac{(\rho C)' - \phi \rho_f C_f}{1-\phi}, \tag{3.17c}$$

$$\sigma_s' = \frac{\sigma' - \phi \sigma_f}{1-\phi}, \tag{3.17d}$$

$$\eta' = \frac{\tilde{J}\eta\tilde{J}^{\dagger}}{\det \tilde{J}}, \tag{3.17e}$$

where $(\rho C)'$ and σ' are given by Eqs. (3.11a) and (3.11b), respectively. Equation (3.17) is the third key result, revealing the theory of transformation complex thermotics in porous media. We only transform the parameters of solids and avoid transforming advection velocities and moving fluids directly. Therefore, the physical problems for experiments have been solved, and the remaining problems are to find practical materials with anisotropic and inhomogeneous thermal conductivities and permeabilities, which have been widely studied based on multilayered structures [33–42].

Figure 3.4a shows the schematic diagram of our experimental suggestion. We use two modules: the heat transfer in porous media and the Darcy law. The left and right boundaries are also set at high pressure (P_L) and low pressure (P_R). We take the wave vector $\beta = 2\pi m/W$ with $m = 10$, and the time period of the thermal wave is $t_0 = 24$ s according to Eq. (3.16) with $\boldsymbol{v}_s = 0$. The initial wavelike temperature field (Fig. 3.4b and f) are the same as those in Fig. 3.2b and e. If there does not exist a cloak coating the obstacle, the thermal wave (Fig. 3.4c and d) and the pressure field (Fig. 3.4e) are strongly distorted. In contrast, a cloak can avoid the distortion of the thermal wave (Fig. 3.4g and h) and the pressure field (Fig. 3.4i). The thermal wave in Fig. 3.4h also has energy loss because of the positive real part of κ. After propagating for one period (24 s), the thermal wave in Fig. 3.4h approximately gains a phase difference of 2π, thus being at the same position as Fig. 3.4f. We also provide experimental suggestions for concentrating and rotating, whose parameters are designed according to Eq. (3.17). The simulation results are shown in Fig. 3.5a–d and e–h, respectively. The concentrating and rotating effects are achieved indeed with a porous media. Therefore, the predictions of Eqs. (3.15)–(3.17) are physical, confirming the validity of transformation complex thermotics in composite materials.

3.5 Conclusion

We have coined a complex thermal conductivity κ and a complex conduction equation (say, complex thermotics) to unify conduction and advection. The real and imaginary parts of κ correspond to conduction and advection, respectively. We have also

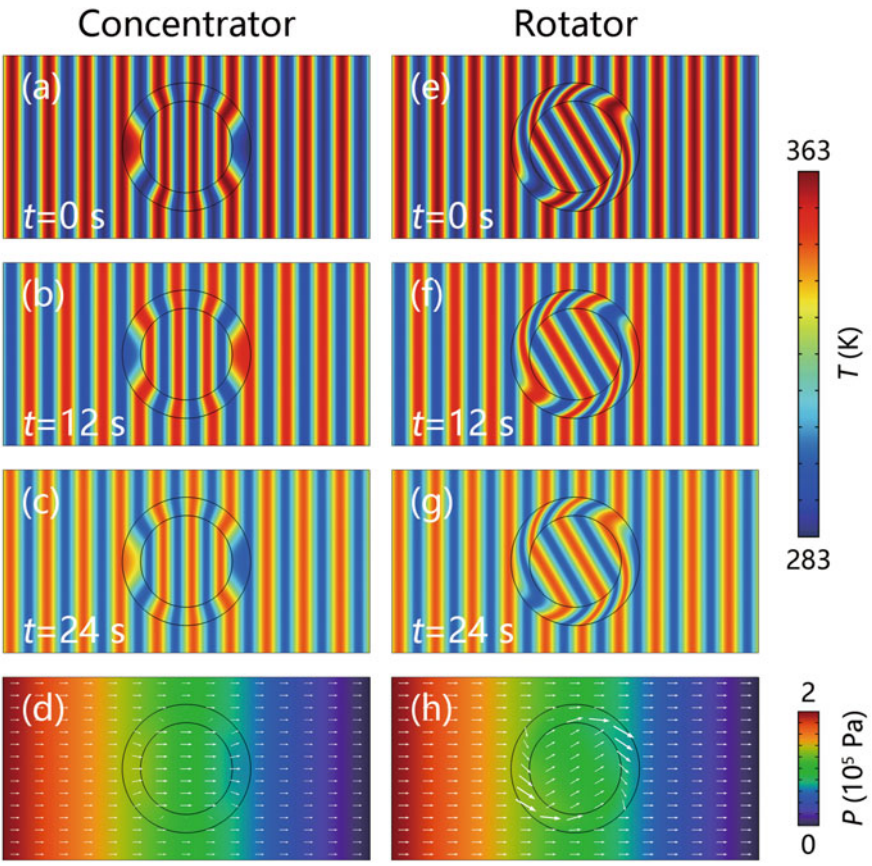

Fig. 3.5 Simulations of **a**–**d** concentrating and **e**–**g** rotating in porous media. The system sizes and background parameters are the same as those for Fig. 3.4. Other parameters are designed with Eq. (3.17). Adapted from Ref. [6]

proved the form-invariance of the complex conduction equation under coordinate transformations and derived the principle for transforming complex thermal conductivities. The current theory allows us to control thermal waves flexibly. Three practical devices have been designed with cloaking, concentrating, and rotating functions. Experimental suggestions are also provided, with the method of weighted average to derive the effective complex thermal conductivities of composite materials such as porous media.

3.6 Exercise and Solution

Exercise

1. Prove that a complex conduction equation can also describe the conduction-advection process in porous media.

Solution

1. The conductive energy density $\boldsymbol{E}_1$ is

$$\boldsymbol{E}_1 = -\sigma \nabla T. \tag{3.18}$$

The advection energy density induced by moving fluids $\boldsymbol{E}_2$ is

$$\boldsymbol{E}_2 = \phi \rho_f C_f \boldsymbol{v}_f T, \tag{3.19}$$

and that induced by moving solids $\boldsymbol{E}_3$ is

$$\boldsymbol{E}_3 = (1-\phi)\, \rho_s C_s \boldsymbol{v}_s T. \tag{3.20}$$

Therefore, the total energy E that flows into the closed surface Σ from time t_1 to t_2 is

$$E = -\int_{t_1}^{t_2} \oiint_{\Sigma} \boldsymbol{n} \cdot (\boldsymbol{E}_1 + \boldsymbol{E}_2 + \boldsymbol{E}_3)\, d\boldsymbol{S} dt = -\int_{t_1}^{t_2} \iiint_{\Omega} \nabla \cdot (\boldsymbol{E}_1 + \boldsymbol{E}_2 + \boldsymbol{E}_3)\, dV dt, \tag{3.21}$$

where Ω is the region enclosed by the surface Σ, $\boldsymbol{n}$ is unit normal vector, dS is the surface element, and dV is the volume element.

On the other hand, the absorbed energy E' can also be derived from the thermodynamic formula

$$E' = \iiint_{\Omega} [\rho C T(t_2) - \rho C T(t_1)]\, dV = \int_{t_1}^{t_2} \iiint_{\Omega} \rho C \left(\frac{\partial T}{\partial t}\right) dV dt. \tag{3.22}$$

According to the law of energy conservation, there must be $E = E'$, and we can derive the energy equation of the conduction-convection process in a porous medium as

$$\rho C \frac{\partial T}{\partial t} + \nabla \cdot \left[-\sigma \nabla T + \phi \rho_f C_f \boldsymbol{v}_f T + (1-\phi)\, \rho_s C_s \boldsymbol{v}_s T\right] = 0. \tag{3.23}$$

With the effective complex thermal conductivity of the porous media (Eq. (3.15)), Eq. (3.23) can be reduced to

$$\rho C \frac{\partial T}{\partial t} + \nabla \cdot (-\kappa \nabla T) = 0. \tag{3.24}$$

Therefore, the conduction-advection process in porous media can be still described by a complex conduction equation where ρC and κ are the weighted average of solids and fluids.

References

1. Guenneau, S., Petiteau, D., Zerrad, M., Amra, C., Puvirajesinghe, T.: Transformed Fourier and Fick equations for the control of heat and mass diffusion. AIP Adv. **5**, 053404 (2015)
2. Dai, G.L., Shang, J., Huang, J.P.: Theory of transformation thermal convection for creeping flow in porous media: cloaking, concentrating, and camouflage. Phys. Rev. E **97**, 022129 (2018)
3. Xu, L.J., Yang, S., Dai, G.L., Huang, J.P.: Transformation omnithermotics: simultaneous manipulation of three basic modes of heat transfer. ES Energy Environ. **7**, 65 (2020)
4. Xu, L.J., Huang, J.P.: Negative thermal transport in conduction and convection. Chin. Phys. Lett. **37**, 080502 (2020)
5. Krešiá, I., Makris, K.G., Leonhardt, U., Rotter, S.: Transforming space with non-Hermitian dielectrics. Phys. Rev. Lett. **128**, 183901 (2022)
6. Xu, L.J., Huang, J.P.: Controlling thermal waves with transformation complex thermotics. Int. J. Heat Mass Transf. **159**, 120133 (2020)
7. Li, Y., Peng, Y.-G., Han, L., Miri, M.-A., Li, W., Xiao, M., Zhu, X.-F., Zhao, J.L., Alù, A., Fan, S.H., Qiu, C.-W.: Anti-parity-time symmetry in diffusive systems. Science **364**, 170 (2019)
8. Cao, P.C., Li, Y., Peng, Y.G., Qiu, C.-W., Zhu, X.-F.: High-Order exceptional points in diffusive systems: robust APT symmetry against perturbation and phase oscillation at APT symmetry breaking. ES Energy Environ. **7**, 48 (2020)
9. Farhat, M., Chen, P.-Y., Bagci, H., Amra, C., Guenneau, S., Alù, A.: Thermal invisibility based on scattering cancellation and mantle cloaking. Sci. Rep. **5**, 9876 (2015)
10. Farhat, M., Guenneau, S., Chen, P.-Y., Alù, A., Salama, K.N.: Scattering cancellation-based cloaking for the Maxwell-Cattaneo heat waves. Phys. Rev. Appl. **11**, 044089 (2019)
11. Fan, C.Z., Gao, Y., Huang, J.P.: Shaped graded materials with an apparent negative thermal conductivity. Appl. Phys. Lett. **92**, 251907 (2008)
12. Chen, T.Y., Weng, C.-N., Chen, J.-S.: Cloak for curvilinearly anisotropic media in conduction. Appl. Phys. Lett. **93**, 114103 (2008)
13. Liu, Y.X., Guo, W.L., Han, T.C.: Arbitrarily polygonal transient thermal cloaks with natural bulk materials in bilayer configurations. Int. J. Heat Mass Transf. **115**, 1 (2017)
14. Guo, J., Qu, Z.G.: Thermal cloak with adaptive heat source to proactively manipulate temperature field in heat conduction process. Int. J. Heat Mass Transf. **127**, 1212 (2018)
15. Qin, J., Luo, W., Yang, P., Wang, B., Deng, T., Han, T.C.: Experimental demonstration of irregular thermal carpet cloaks with natural bulk material. Int. J. Heat Mass Transf. **141**, 487 (2019)
16. Dede, E., Nomura, T., Lee, J.: Thermal-composite design optimization for heat flux shielding, focusing, and reversal. Struct. Multidiscip. Optim. **49**, 59 (2014)
17. Fujii, G., Akimoto, Y., Takahashi, M.: Exploring optimal topology of thermal cloaks by CMA-ES. Appl. Phys. Lett. **112**, 061108 (2018)
18. Fujii, G., Akimoto, Y.: Topology-optimized thermal carpet cloak expressed by an immersed boundary level-set method via a covariance matrix adaptation evolution strategy. Int. J. Heat Mass Transf. **137**, 1312 (2019)
19. Fujii, G., Akimoto, Y.: Optimizing the structural topology of bifunctional invisible cloak manipulating heat flux and direct current. Appl. Phys. Lett. **115**, 174101 (2019)
20. Zhou, L.L., Huang, S.Y., Wang, M., Hu, R., Luo, X.B.: While rotating while cloaking. Phys. Lett. A **383**, 759 (2019)
21. Tsai, Y.-L., Li, J.Y., Chen, T.Y.: Simultaneous focusing and rotation of a bifunctional thermal metamaterial with constant anisotropic conductivity. J. Appl. Phys. **126**, 095103 (2019)

22. Urzhumov, Y.A., Smith, D.R.: Fluid flow control with transformation media. Phys. Rev. Lett. **107**, 074501 (2011)
23. Urzhumov, Y.A., Smith, D.R.: Flow stabilization with active hydrodynamic cloaks. Phys. Rev. E **86**, 056313 (2012)
24. Bowen, P.T., Urzhumov, Y.A., Smith, D.R.: Wake control with permeable multilayer structures: the spherical symmetry case. Phys. Rev. E **92**, 063030 (2015)
25. Park, J., Youn, J.R., Song, Y.S.: Hydrodynamic metamaterial cloak for drag-free flow. Phys. Rev. Lett. **123**, 074502 (2019)
26. Park, J., Youn, J.R., Song, Y.S.: Fluid-flow rotator based on hydrodynamic metamaterial. Phys. Rev. Appl. **12**, 061002 (2019)
27. Wang, Z.Y., Li, C.Y., Zatianina, R., Zhang, P., Zhang, Y.Q.: Carpet cloak for water waves. Phys. Rev. E **96**, 053107 (2017)
28. Li, C.Y., Xu, L., Zhu, L.L., Zou, S.Y., Liu, Q.H., Wang, Z.Y., Chen, H.Y.: Concentrators for water waves. Phys. Rev. Lett. **121**, 104501 (2018)
29. Zou, S.Y., Xu, Y.D., Zatianina, R., Li, C.Y., Liang, X., Zhu, L.L., Zhang, Y.Q., Liu, G.H., Liu, Q.H., Chen, H.Y., Wang, Z.Y.: Broadband waveguide cloak for water waves. Phys. Rev. Lett. **123**, 074501 (2019)
30. Li, Y., Zhu, K.-J., Peng, Y.-G., Li, W., Yang, T.Z., Xu, H.-X., Chen, H., Zhu, X.-F., Fan, S.H., Qiu, C.-W.: Thermal meta-device in analogue of zero-index photonics. Nat. Mater. **18**, 48 (2019)
31. Xu, L.J., Huang, J.P.: Chameleonlike metashells in microfluidics: a passive approach to adaptive responses. Sci. China-Phys. Mech. Astron. **63**, 228711 (2020)
32. Bear, J., Corapcioglu, M.Y.: Fundamentals of Transport Phenomena in Porous Media. Springer, Netherlands (1984)
33. Vemuri, K.P., Bandaru, P.R.: Geometrical considerations in the control and manipulation of conductive heat flux in multilayered thermal metamaterials. Appl. Phys. Lett. **103**, 133111 (2013)
34. Yang, T.Z., Vemuri, K.P., Bandaru, P.R.: Experimental evidence for the bending of heat flux in a thermal metamaterial. Appl. Phys. Lett. **105**, 083908 (2014)
35. Vemuri, K.P., Canbazoglu, F.M., Bandaru, P.R.: Guiding conductive heat flux through thermal metamaterials. Appl. Phys. Lett. **105**, 193904 (2014)
36. Shang, J., Wang, R.Z., Xin, C., Dai, G.L., Huang, J.P.: Macroscopic networks of thermal conduction: Failure tolerance and switching processes. Int. J. Heat Mass Transf. **121**, 321 (2018)
37. Xu, L.J., Yang, S., Huang, J.P.: Thermal theory for heterogeneously architected structure: fundamentals and application. Phys. Rev. E **98**, 052128 (2018)
38. Xu, L.J., Yang, S., Huang, J.P.: Thermal transparency induced by periodic interparticle interaction. Phys. Rev. Appl. **11**, 034056 (2019)
39. Li, J.X., Li, Y., Li, T.L., Wang, W.Y., Li, L.Q., Qiu, C.-W.: Doublet thermal metadevice. Phys. Rev. Appl. **11**, 044021 (2019)
40. Xu, L.J., Huang, J.P.: Metamaterials for manipulating thermal radiation: Transparency, cloak, and expander. Phys. Rev. Appl. **12**, 044048 (2019)
41. Dai, G.L., Huang, J.P.: Nonlinear thermal conductivity of periodic composites. Int. J. Heat Mass Transf. **147**, 118917 (2020)
42. Huang, J.P.: Theoretical Thermotics: Transformation Thermotics and Extended Theories for Thermal Metamaterials. Springer, Singapore (2020)